Phase transition in organic–inorganic perovskite (C 9 H 19 NH 3) 2 PbI 2 Br 2 of long-chain alkylammonium

ARTICLE *in* RESULTS IN PHYSICS · APRIL 2012

DOI: 10.1016/j.rinp.2012.04.003

Results in Physics 2 (2012) 71–76

Contents lists available at SciVerse ScienceDirect

Results in Physics

journal homepage: www.journals.elsevier.com/results-in-physics

Phase transition in organic–inorganic perovskite $(C_9H_{19}NH_3)_2$ PbI_2Br_2 of long-chain alkylammonium

H. Abid [a,b,*], A. Trigui [a], A. Mlayah [c], E.K. Hlil [b], Y. Abid [a]

[a] Laboratoire de Physique Appliquée, Faculté des sciences, Université de Sfax, Tunisia
[b] Institut Néel, CNRS et Université Joseph Fourier, BP 166, F-38042 Grenoble Cedex 9, France
[c] Centre d'Elaboration de Matériaux et d'Etudes Structurales (CEMES), CNRS—Université de Toulouse, 29 rue Jeanne Marvig, 31055 Toulouse, France

ARTICLE INFO

Article history:
Received 23 January 2012
Accepted 24 April 2012
Available online 3 May 2012

Keywords:
Organic-Inorganic perovskites
X-ray Diffraction versus temperature
Differential Scanning Calorimetry (DSC)FT-Raman
ab initio MP3 method
Phase transition

ABSTRACT

Single perovskite slab alkylammonium lead iodides bromides $(C_9H_{19}NH_3)_2PbI_2Br_2$ is a new member of the family of hybrid organic-inorganic perovskite compounds. It exhibits a single structural phase transition with changes in the conformation of alkylammonium chains below room temperature. Differential scanning calorimetry (DSC), powder X-ray diffraction and FT-Raman spectroscopy were used to investigate this phase transition. These changes were characterized by a decreased conformational disorder of the methylene units of the alkyl chains. Phase transition was examined in light of the interesting optical properties of this material, as well as the relevance of this system as models for phase transitions in lipid bilayers.

1. Introduction

Layered organic–inorganic hybrid compounds have been widely studied [1], since they can, in principle, combine properties of the inorganic and organic parts within a single system. In the molecular hybrids of interest, organic groups are interleaved between inorganic sheets and held in place either by covalent or ionic bonding [2]. The majority of the organic–inorganic molecular composites that have been studied so far derive from the layered perovskite structure and comprise inorganic perovskite sheets MX_4:(M = Pb, Sn, Bi, .. and X = I, Br, Cl...) alternating with either a double-layer of organic primary ammonium cations $(C_nH_{2n+1}NH_3)_2$ or a single layer of organic diammonium cations $(NH_3(CH_2)_nNH_3)_2$ [3]. Such molecules are considered as important materials because their intrinsic organic (insulating)-inorganic (semiconducting) structures are akin to "natural quantum-well" architectures [4–7]. Associated with these quantum-well structures are tunable excitonic properties that depend crucially on the dielectric properties, governed usually by the chain length of the insulating organic layer [7,8]. Applications of such materials include the development of functional magnetic [2], electronic [9] and optoelectronic [10] materials.

An understanding of phase transitions in the organic part of these hybrid structures is quite important from materials point of view. In addition, because lipid bilayers are ubiquitous in the natural world, it is of great interest to study phase transition in model systems that share similarities with lipid bilayers. Long chain alkyl ammonium layered perovskites share similarity with phospholipids bilayers that are known to undergo structural phase transitions with temperature.

However, unlike lipid bilayers where individual molecules can undergo lateral diffusion and also flip-flop between layers, the alkyl chain bilayers in hybrid compounds have one end firmly anchored to the inorganic sheet that is quite rigid and therefore are characterized by total absence of translational mobility. In the temperature range of interest, the inorganic lattice undergoes no change. The degrees of freedom of the alkyl chains of the anchored alkyl chain bilayers in these hybrid materials are restricted to changes in conformation. A closely related and extensively studied system is the self-assembled monolayers on even surfaces [11–15].

Many inorganic–organic hybrid systems based on the layered perovskite structure are known to exhibit one or more phase transitions versus temperature [16–22]. Most studies have concluded that the main transition taking place at higher temperatures is a melting of the alkyl chains. The low temperature transition, exhibited by some of these compounds, is a dynamic disordering of the rigid alkyl moieties.

In this study, we report a detailed investigation of the thermal behavior of the alkyl chains in $(C_9H_{19}NH_3)_2PbI_2Br_2$ compound. The techniques used include differential scanning calorimetry (DSC), powder X-ray diffraction (XRD), IR spectroscopy, and Raman spectroscopy. The XRD and Raman spectroscopy studies have been carried out as a function of temperature. This combination of techniques allowed us to examine in detail the precise nature of the

* Corresponding author at: Laboratoire de Physique Appliquée, Faculté des sciences, Université de Sfax, Tunisie. Tel.: +216 21 121192; fax: +216 74 274437.
E-mail address: haithamlpa@yahoo.fr (H. Abid).

2211-3797/$ - see front matter © 2012 Elsevier B.V. All rights reserved.
http://dx.doi.org/10.1016/j.rinp.2012.04.003

phase transition to relate changes in the crystal lattice with changes in the conformation of the alkylammonium chains.

2. Experimental section

The ($C_9H_{19}NH_3I$) precipitates are first formed by adding an aqueous solution of HI (aqueous solution, 57%) to nonylamine ($C_9H_{19}NH_2$). Next, ($C_9H_{19}NH_3^+I^-$)/$PbBr_2$ in a molar ratio of 2:1 are dissolved in N, N-dimethylformamide (DMF). The obtained solution is kept at room temperature. Two weeks later, platelets crystals were formed. The purity of the solution was improved by second re-crystallization. The overall reaction may be written as:

$$CH_3-(CH_2)_8-NH_2+HI\rightarrow[CH_3-(CH_2)_8-NH_3]^+I^-$$

$$2[[CH_3-(CH_2)_8-NH_3]^+I^-]+PbBr_2\rightarrow[CH_3-(CH_2)_8-NH_3]_2PbI_2Br_2$$

The thermal behavior of this compound was investigated by differential scanning calorimetry using a Perkin-Elmer DSC 2C instrument operated at a scanning rate of 5 K min^{-1} under an N_2 atmosphere. The temperature scale was calibrated using a mercury (Hg) standard (T_m = 234.1 K). Powder X-ray diffraction patterns versus temperature were acquired on a Shimadzu XD-D1 diffractometer operated in the θ–2θ Bragg-Brentano geometry. Samples were mounted on glass block that could be heated in a controlled manner. IR spectra of the title compound were recorded as KBr pellets on a Perkin-Elmer spectrum 2000 operating at 4 cm^{-1} resolution. FT-Raman spectra were recorded on a Dilor XY spectrometer using an Argon laser (488 nm) for excitation. Spectra were recorded at a resolution of 4 cm^{-1}.

3. Results and discussion

Fig. 1 shows schematic structures of $(C_9H_{19}NH_3)_2PbI_2Br_2$ compound. The salient features of these long chain alkylammonium lead iodides-bromides follow: (1) the inorganic portions of the structure remain invariant when the number of carbon atoms in the alkylammonium chains is changed. This is verified from the 1-D projections of the electron densities obtained from a Fourier transforms of the 00*l* reflections in the XRD patterns [23]. (2) The alkylammonium chains are all-trans at room temperature [24]. (3) Organic chains fill inters slabs spacing formed by succession of tow inorganic layers and form N–H···I hydrogen bonds to I atoms of different PbI_2Br_2 octahedra through each terminal ammonium group. In such a packing, the organic moieties form an insulator barrier separating the semiconductor PbI_2Br_2 layers. This periodic structure can be regarded as an organic-inorganic self-organized quantum well structure.

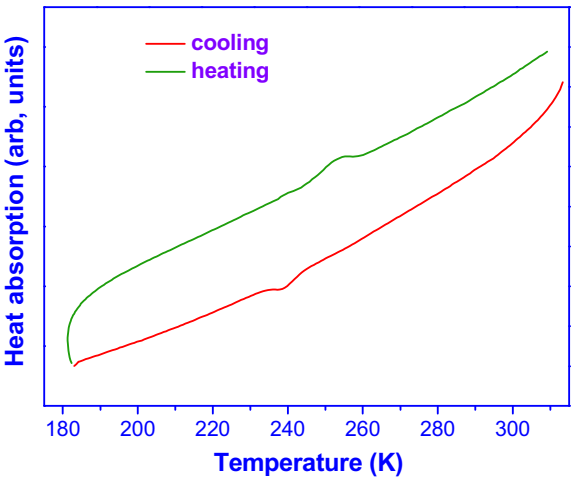

Fig. 2. DSC trace of $(C_9H_{19}NH_3)_2PbI_2Br_2$ compound.

Here, our aim is not to distinguish between one of two possible structures displayed in Fig. 1 one structure with opposed organic chains and second structure with organic chains forming herringbone pattern, but rather, to report the temperature dependence of the structure, with a focus on what happens to the conformation and disposition of the organic moieties when the temperature is dropped.

3.1. Differential scanning calorimetry (DSC)

The differential scanning calorimetric traces of $(C_9H_{19}NH_3)_2PbI_2Br_2$ compound is shown in Fig. 2. On cooling, we observe one exotherm transition around 230 K corresponding to first-order phase transition. When the sample is heated, we observe one endotherm, corresponding to the transition of the cooling run but at a higher temperature.

3.2. Powder X-ray diffraction

Structural information at room temperature has been mentioned elsewhere [25]. In summary, the title compound crystallizes in perovskite type monolayered structure with space group $P2_1/m$ (Z = 2) with a = 25.2331 Å, b = 8.8441 Å, c = 23.0031 Å, and β = 104.01401°. The parameter c is related to the interlayer distance,

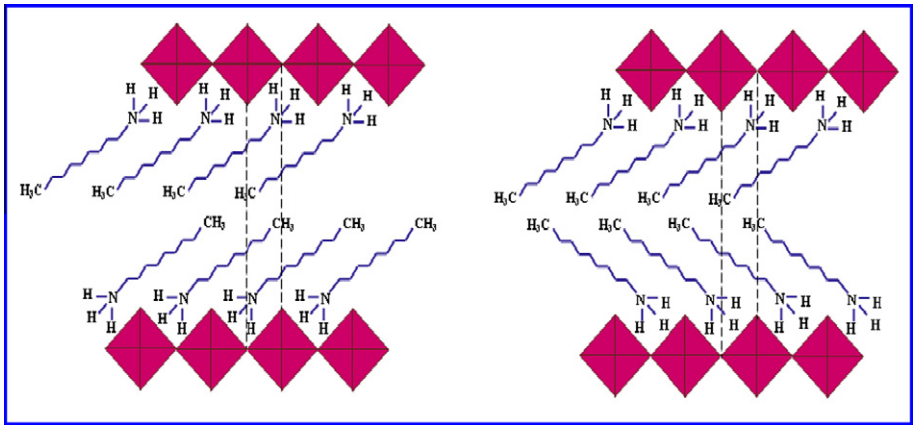

Fig. 1. Schematic depicting the two possible structures of the alkyl chains in the layered $(C_9H_{19}NH_3)_2PbI_2Br_2$.

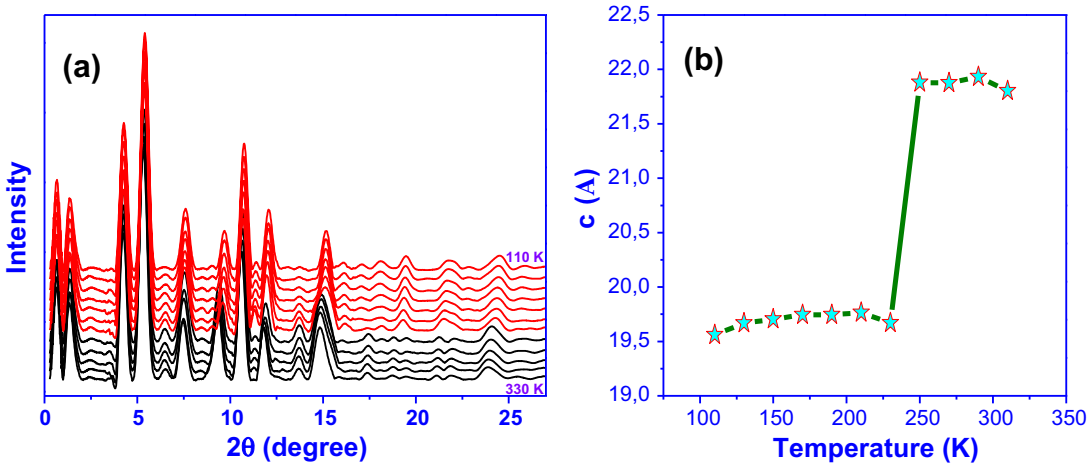

Fig. 3. (a) X-ray diffraction patterns of $(C_9H_{19}NH_3)_2PbI_2Br_2$ at different temperatures between 330 and 110 K at intervals of 20 K and (b) the interlayer spacing of $(C_9H_{19}NH_3)_2PbI_2Br_2$ at different temperatures.

a and *b* are in parallel to the plane of the layers. The main characteristic of this structure is a strong spontaneous distortion of the PbI_4Br_2 octahedra. This explains well the crystallization on monoclinic cell symmetry. Fig. 3a displays the temperature dependence of the powder X-ray diffraction pattern for $(C_9H_{19}NH_3)_2PbI_2Br_2$ compound. Because of the highly lamellar nature of this family compounds, the XRD patterns reveal only 0 0 *l* reflections [7], which were indexed as 001, 003, 005, 007, ... The data were recorded from a temperature 330 K to 110 K at intervals of 20 K. One phase transition has been shown characterized by discontinuous evolution of the powder data; indeed, large changes occur around $T = 230$ K. This suggests a first-order character of transition. The peaks are noticeably shifted to the higher Bragg angle, corresponding to lattice contraction along the *c*-axis decreased inter-inorganic slab spacing. The change in the *c* crystallographic parameter as a function of temperature is displayed in Fig. 3b.

3.3. Vibrational spectroscopic studies

In order to gain more information on the crystal dynamics, on the degree of disorder and on the mechanisms involved in the transition, we have undertaken a Raman study between 293 and 113 K.

Before addressing phase transition study, it is necessary to obtain a reliable assignment of the IR and Raman bands at room temperature. The vibrational features consist of well-separated peaks which can be subdivided in two main groups: (1) the vibrational modes of Pb–I and Pb–Br octahedra forming the two-dimensional layers appear in the low-wavenumber region 50–200 cm^{-1}, and (2) the internal modes of the organic cations occur at higher wavenumbers 200–4000 cm^{-1}.

Optimal geometry and the vibrational wavenumbers of both the organic and the inorganic components were calculated. We have considered the Cluster built with six PbI_4Br_2 octahedra sharing their corner and four organic cations were considered as seen in Fig. 4. For optimal geometry calculations, structural parameters obtained from the X-ray data [25] were used as initial inputs. Geometry optimization was performed using the PM3 method implemented in Gaussian 98 program package [26] without any symmetry or parameters constraints (symmetry C1). All vibration wavenumbers were found to be real and positive. Graphic viewer MOLDEN 3.8 [27] was used to display the vibration eigen-modes. The calculated wavenumbers were rescaled by a factor (0.9761) following Radom and Scott [28]. As can be seen, the optimal geometry is very close to the experimental one [25]. The infrared

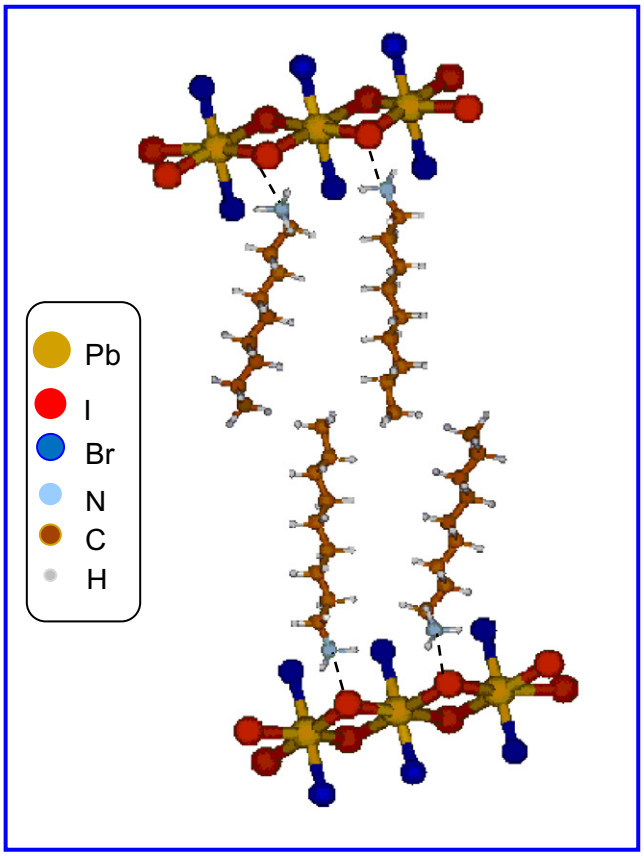

Fig. 4. Geometry of a cluster model optimized using the PM3 method.

spectrum measured between 400 and 4000 cm^{-1} is shown in Fig. 5. In (Fig. 6a–c) are presented the Raman spectra of $(C_9H_{19}NH_3)_2PbI_2Br_2$ crystals recorded at room temperature. Calculated wavenumbers and observed IR and Raman bands are listed in Table 1. Proposed assignments of the main spectral features are summarized in this table. However, by comparison with previous works reported on similar compounds [29–32], we can distinguish between the Raman bands corresponding to the PbI_2Br_2 octahedral motion and those associated with the C_9 chains. As seen, two intense bands located at 109 and 143 cm^{-1} are visible in the Raman spectra. According to the calculated wavenumbers, both bands

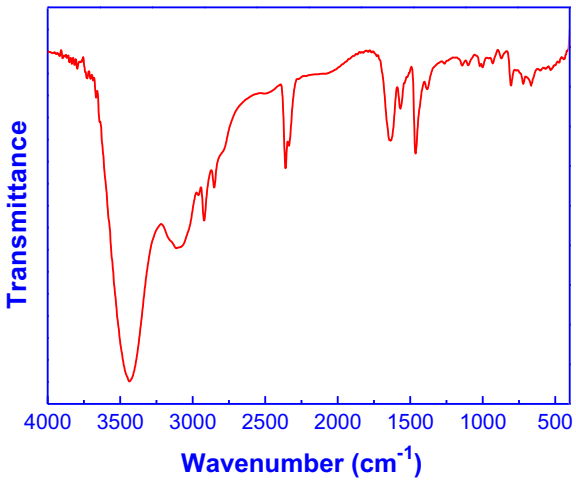

Fig. 5. Infrared spectrum of $(C_9H_{19}NH_3)_2PbI_2Br_2$ compound at room temperature.

could be assigned to the [υ(Pb–I) and υ(Pb–Br)] stretching vibration of the Pb–I and Pb–Br bonds in the inorganic chains. The bands observed between 400 and 3500 cm^{-1} in the Raman and Infrared spectra are assigned to internal modes of organic cation. The difference between the calculated and measured wavenumbers in Table 1 is mainly due to the small orbital basis set of the PM3 method.

Vibrational spectroscopy has been extensively used for probing conformation of alkyl chain. The intense bands that appear between 2800 and 3100 cm^{-1} are the C–H stretching modes of the methyl and methylene groups of the alkyl chains. The peak at 2809 cm^{-1} observed in Raman and expected in IR spectra is assigned to the symmetric stretching $\upsilon_s(CH_2)$ mode of the methylene groups, the antisymmetric $\upsilon_a(CH_2)$ stretching mode appear at 2858 and 2851 cm^{-1} respectively in Raman and IR spectra . The peaks at 2960 cm^{-1} and 2961 cm^{-1} observed respectively in Raman and IR spectra are assigned to the symmetric $\upsilon_s(CH_3)$ stretching of the methyl groups, the methyl antisymmetric stretching $\upsilon_a(CH_3)$ mode appear at 3024 cm^{-1} in Raman and at 3085 cm^{-1} in IR spectra at 3100 cm^{-1}. The alkylammonium chains are all-trans at room temperature [24]. It is well-known that the methylene stretching mode frequencies are sensitive to the conformation of the alkyl chain shifting to lower frequencies with decreased conformational gauche disorder [33,34]. The observed peak positions of the symmetric and antisymmetric C–H stretching modes of the methylene groups in $(C_9H_{19}NH_3)_2PbI_2Br_2$ compound indicate that, at room temperature, the alkyl chains are essentially in an all-trans conformation.

The observed peaks at 806 cm^{-1} in Raman and 798 cm^{-1} in IR spectra are assigned to the $\rho(CH_2)$ rocking vibration, and the fact that this band as well as the $\delta(CH_2)$ scissoring mode at 1458 cm^{-1} and 1462 cm^{-1} respectively in Raman and IR spectra appear as singlets implies monoclinic sub-cell packing. These bands are known to split into two distinct components as a result of crystal or factor-group splitting in hexagonal or monoclinic packing [35,36]. Compared with homologous compounds those found in the literature [23,24], spectroscopic measurements show that at room temperature the alkyl ammonium chains are arranged with all alkyl chains adopting a planar all-trans conformation. The latter was established from an analysis of the progression band series in the infrared and Raman spectroscopy of $(C_9H_{19}NH_3)_2PbI_2Br_2$. The progression band series indicate that all CH_2 units are in trans-registry at room temperature and provide a characteristic signature for alkyl chains that adopt an all-trans conformation.

Decrease in temperature induces changes in alkyl chain conformation. The methylene stretching modes that are sensitive to chain conformation shift abruptly around 230 K to lower frequencies corresponding to the phase transition. The Raman spectra of

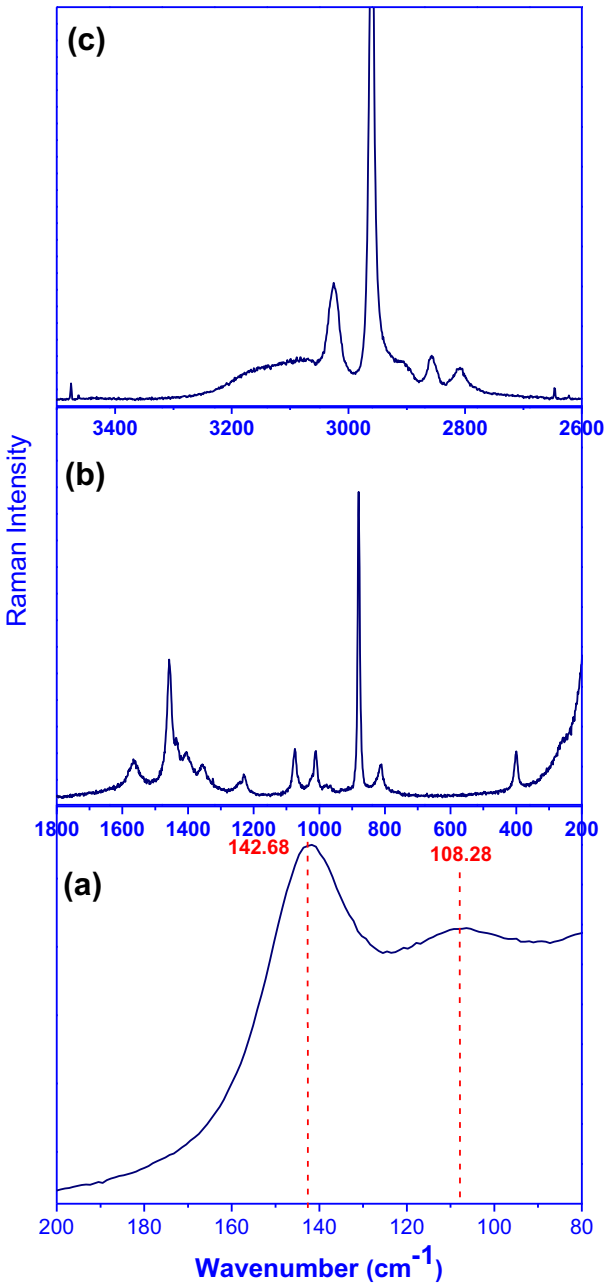

Fig. 6. Raman spectra of $(C_9H_{19}NH_3)_2PbI_2Br_2$ compound in the (a) 200–80 cm^{-1}, (b) 1800–200 cm^{-1} and (c) 3500–2600 cm^{-1} wavenumber region at room temperature.

$(C_9H_{19}NH_3)_2PbI_2Br_2$ at different temperatures are shown in Fig. 7. We observe an abrupt shift of the methylene C–H stretching frequencies, both ν_s and ν_a, to lower wavenumbers at the temperature corresponding to the exotherm in the DSC.

Refinement of the powder (XRD) pattern in (303–113 K) temperature range confirms the phase change expected by DSC measurements. Indeed, it showed one first-order phase transition around 230 K due to changes in lattice parameters (*a, b, c* and β) without change of space group or crystal system.

Fig. 3b displays variation of the parameter *c* as the temperature decreases. This parameter shows a sharp decrease close the transition temperature (230 K). Such decrease induces both noticeable abrupt shift to lower frequencies of peaks position corresponding to symmetric and antisymmetric C–H stretching (Fig. 8a); and intensity decrease of the C–H stretching. This intensity remains

Table 1
Measured and calculated vibration wavenumbers (cm^{-1}) of $(C_9H_{19}NH_3)_2PbI_2Br_2$ compound and proposed assignments of the observed Raman and IR bands.

Observed wavenumbers (cm^{-1})		Calculated wavenumbers (cm^{-1})	Proposed assignments
Raman	IR		
109	–	126	ν (Pb–I) Stretching
143	–	159	ν (Pb–Br) Stretching
401	435	408	(C–C–N) Bending
–	580	546	(C–C–C) Bending
815	805	818	ν (C–C) Stretching
883	871	864	ρ (NH_3) rocking
1010	1002	1010	ρ (CH_2) Rocking
1075	1087	1090	ρ (CH_3) Rocking
–	1101	1113	ν (C–N) Stretching
1230	–	1239	τ (CH_2) Twisting
1355	1381	1374	ω (CH_2) Wagging
1458	1463	1472	δ (CH_2) Scissoring
1565	1566	1406	δ (NH_3) Deformation
	1637	1651	δ (NH_3) Scissoring
2809	–	2835	ν_s (CH_2) symmetric stretching
2858	2851	2889	ν_a (CH_2) Antisymmetric stretching
2960	2961	2962	ν_s (CH_3) Symmetric stretching
3024	3085	3102	ν_a (CH_3) Antisymmetric stretching
–	3430	3419	ν (NH) stretching

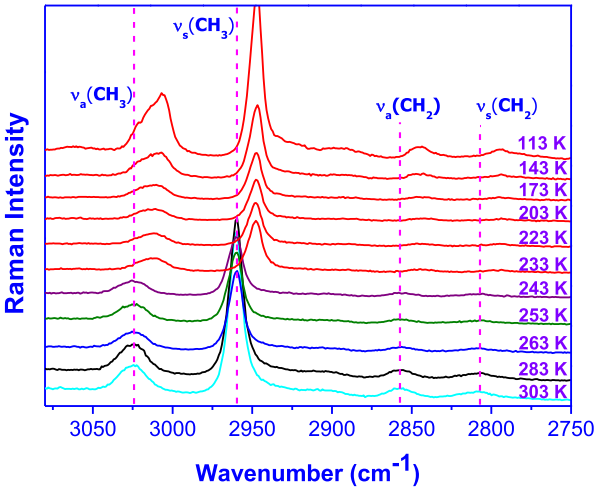

Fig. 7. Raman spectra of $(C_9H_{19}NH_3)_2PbI_2Br_2$ in the C–H stretching region at different temperature between 303 and 113 K.

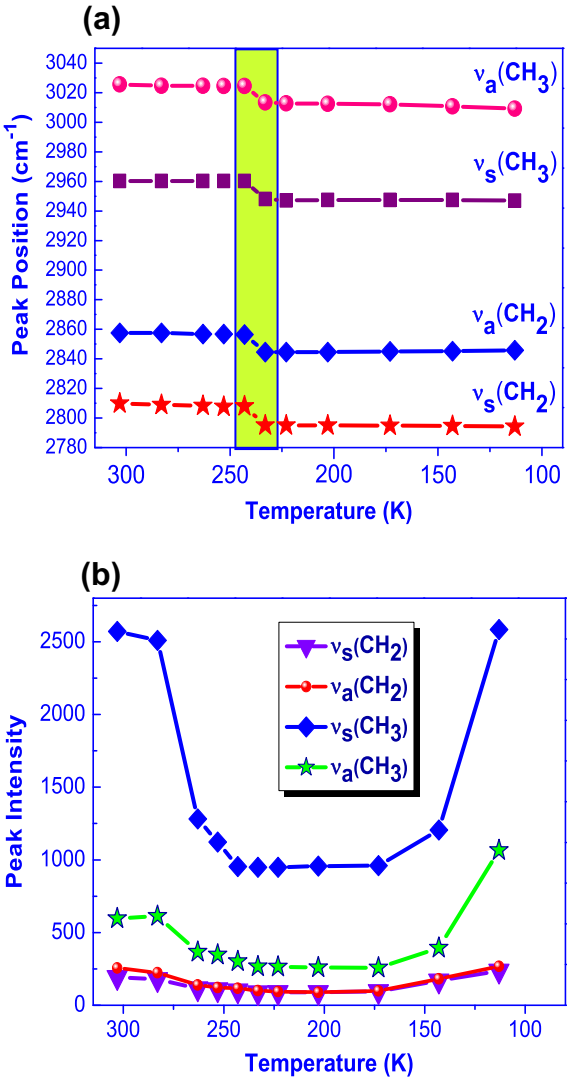

Fig. 8. (a) Peak position of the methylene C–H stretching at different temperatures between 303 K and 113 K and (b) peak intensity of the methylene C–H stretching at different temperatures between 303 K and 113 K.

constant when the temperature is comprised between 230 and 173 K. Lower to 173 K, increase of this intensity and a slight shift of the methyl anti-symmetric stretching $\nu_a(CH_3)$ mode to lower frequencies is observed (Fig. 8b).

To better understand the structure behavior after the temperature transition, we have plotted (*a, b* and β) parameter variations versus temperature (Fig. 9a–c). The *a*-axis increases sharply during the transition and the *b* lattice parameter decreases slightly causing a remarkable increase of the β angle. This should be explained by the fact that when the *c* parameter decreases, organic chains are close to each other causing the *a* increase, *b* decrease and consequently β angle increase. These changes should cause a slight lattice distortion. Furthermore, just below temperature phase transition, the intensity of organic chains vibrational modes is stabilized by adopting the new phase. All structure changes are characterized by a decreased conformational disorder of the methylene units of the alkyl chains and gain of tilt angle coherence (from the normal to the inorganic layers) leading to a decrease in the inter slabs spacing. In addition, the intensity increases again below the

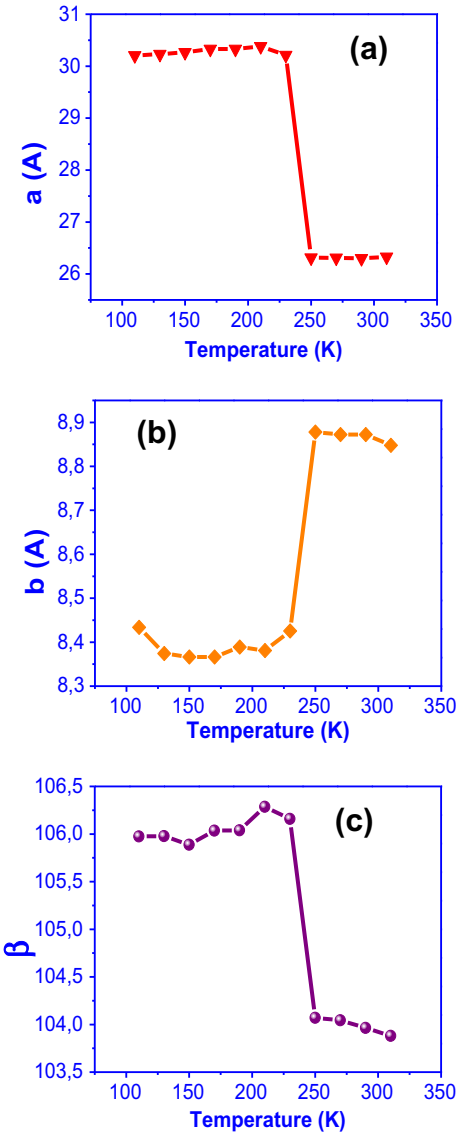

Fig. 9. (a) Variation of *a* parameter as a function of temperature (b) variation of *b* parameter as a function of temperature and (c) variation of the title angle *β* parameter as a function of temperature.

temperature 173 K which is due probably to that different organic chains vibrational modes taking place in the plane (*ab*).

4. Conclusion

The layered organic-inorganic hybrid perovskite $(C_9H_{19}NH_3)_2PbI_2Br_2$ is composed of alkyl ammonium chains anchored to PbI_2Br_2 inorganic slabs. With the decrease of temperature, the $(C_9H_{19}NH_3)_2PbI_2Br_2$ compound exhibits a first-order phase transition accompanied by an increase in inters slabs spacing. This transition is characterized by a decreased conformational disorder of the methylene units of the chain and gain of tilt angle coherence leading to an increase in the inter slabs spacing.

References

[1] Mitzi DB. Prog Inorg Chem 1999;48:1.
[2] Philos DP, Trans R. Soc London A 1985;314:145.
[3] Papavassiliou GC. Prog Solid State Chem 1997;25:125.
[4] Mitzi DB, Field CA, Harrison WTA, Guloy AM. Nature 1994;369:467.
[5] Papavassiliou GC, Koutselas IB, Terzis A, Whangbo MH. Solid State Commun 1994;91:695.
[6] Ishihara T, Takahashi J, Goto T. Solid State Commun 1989;69:933.
[7] Ishihara T, Takahashi J, Goto T. Phys Rev B 1990;42:11099.
[8] Hong X, Ishihara T, Nurmikko AV. Phys ReV B 1992;45:6961.
[9] Kagan CR, Mitzi DB, Dimitrakopoulos CD. Science 1999;286:945.
[10] Kataoka T, Kondo T, Ito R, Sasaki S, Uchida K, Miura N. Physics B 1994;201:423.
[11] Heinz H, Vaia RA, Krishnamoorti R, Farmer BL. Chem Mater 2007;19:59.
[12] Heinz H, Vaia RA, Farmer BL. J Chem Phys 2006;124:224713.
[13] Maged OA, Ploetze M, Skrabal P. J Phys Chem B 2004;108:2580.
[14] Heinz H, Suter UW. Chem Int Ed 2004;43:2239.
[15] Heinz H, Castelijns HJ, Suter UW. J Am Chem Soc 2003;155:9500.
[16] Salerno V, Grieco A, Vacatello M. J Phys Chem 1976;22:2444.
[17] Blinc R, Burgar M, Lozar B, Seliger J, Slak J, Rutar V, Arend H, Kind R. J Chem Phys 1977;66:278.
[18] Kind R, Plesko S, Arend R, Blind R, Zeks B, Seliger J, Lozar B, Slak J, Levstik C, Filipic C, Zagar V, Lahajnar G, Milia F, Chapuis G. J Chem Phys 1979;71:2118.
[19] Needham GF, Willett RD, Franzen HF. J Phys Chem 1981;85:3385.
[20] Needham GF, Willett RD, Franzen HF. J Phys Chem 1984;88:674.
[21] Casal HL, Cameron DG, Mantsch HH. J Phys Chem 1985;85:5557.
[22] Almirrante C, Minoni G, Zerbi G. J Phys Chem 1986;90:852.
[23] Venkataraman NV, Bhagyalakshmi S, Vasudevan S, Seshadri R. Phys Chem Phys 2002;4:4553.
[24] Venkataraman NV, Barman S, Vasudevan S, Seshadri R. Chem Phys Lett 2002;358:139.
[25] Abid H, Samet A, Dammak T, Mlayah A, Hlil EK, Abid Y. J Lumin 2011;131:1753.
[26] Frisch MJ, Truuck GW, Schlegel HB, Scuseria GE, Robb MA, Cheeseman JR, et al. Gaussian 98 Revision A.5. Gaussian: Pittsburgh, 1998.
[27] Noordik JH, Schaftenaar G. J Comput Aided Mol Des 2000;14:123.
[28] Radom L, Scott AP. J Phys Chem 1996;100:16502.
[29] Abid Y. J Phys Condens Matter 1994;33:119.
[30] Abid Y, Kamoun M, Daoud A, Romain F. Phase Transit 1992;40:239.
[31] Elleuch S, Abid Y, Mlayah A, Boughzala H. J Raman Spectrosc 2008;39:786.
[32] Dammak T, Elleuch S, Bougzhala H, Mlayah A, Chtourou R, Abid Y. J Lumin 2009;129:893.
[33] MacPhail RA, Strauss HL, Snyder RG, Elliger CA. J Phys Chem 1984;88:334.
[34] Snyder RG, Strauss HL, Elliger CA. J Phys Chem 1982;86:5145.
[35] Snyder RG. J Mol Spectrosc 1961;7:116.
[36] Uno T, Machida K, Miyajima K. Spectrochim Acta 1968;24A:1749.